



# Exogenous GDF11 attenuates non-canonical TGF- $\beta$ signaling to protect the heart from acute myocardial ischemia–reperfusion injury

Hsing-Hui Su<sup>1</sup> · Jiuan-Miaw Liao<sup>2</sup> · Yi-Hsin Wang<sup>3</sup> · Ke-Min Chen<sup>4</sup> · Chia-Wei Lin<sup>5</sup> · I-Hui Lee<sup>6,7</sup> · Yi-Ju Li<sup>8,9</sup> · Jing-Yang Huang<sup>3,10</sup> · Shen Kou Tsai<sup>11</sup> · Jiin-Cherng Yen<sup>1</sup> · Shiang-Suo Huang<sup>3,12,13</sup> 

Received: 15 February 2019 / Accepted: 14 March 2019 / Published online: 21 March 2019  
© Springer-Verlag GmbH Germany, part of Springer Nature 2019

## Abstract

Growth differentiation factor 11 (GDF11) is a member of the transforming growth factor beta 1 (TGF- $\beta$ 1) superfamily that reverses age-related cardiac hypertrophy, improves muscle regeneration and angiogenesis, and maintains progenitor cells in injured tissue. Recently, targeted myocardial delivery of the *GDF11* gene in aged mice was found to reduce heart failure and enhance the proliferation of cardiac progenitor cells after myocardial ischemia–reperfusion (I–R). No investigations have as yet explored the cardioprotective effect of exogenous recombinant GDF11 in acute I–R injury, despite the convenience of its clinical application. We sought to determine whether exogenous recombinant GDF11 protects against acute myocardial I–R injury and investigate the underlying mechanism in Sprague–Dawley rats. We found that GDF11 reduced arrhythmia severity and successfully attenuated myocardial infarction; GDF11 also increased cardiac function after I–R, enhanced HO-1 expression and decreased oxidative damage. GDF11 activated the canonical TGF- $\beta$  signaling pathway and inactivated the non-canonical pathways, ERK and JNK signaling pathways. Moreover, administration of GDF11 prior to reperfusion protected the heart from reperfusion damage. Notably, pretreatment with the activin-binding protein, follistatin (FST), inhibited the cardioprotective effects of GDF11 by blocking its activation of Smad2/3 signaling and its inactivation of detrimental TGF- $\beta$  signaling. Our data suggest that exogenous GDF11 has cardioprotective effects and may have morphologic and functional recovery in the early stage of myocardial I–R injury. GDF11 may be an innovative therapeutic approach for reducing myocardial I–R injury.

**Keywords** Growth differentiation factor 11 · Transforming growth factor beta 1 · Myocardial ischemia–reperfusion · Smad2/3 · TGF- $\beta$  non-canonical pathway

**Electronic supplementary material** The online version of this article (<https://doi.org/10.1007/s00395-019-0728-z>) contains supplementary material, which is available to authorized users.

- ✉ Shen Kou Tsai  
ch9198@chgh.org.tw
- ✉ Jiin-Cherng Yen  
jcyen@ym.edu.tw
- ✉ Shiang-Suo Huang  
sshuang@csmu.edu.tw

Extended author information available on the last page of the article

## Introduction

The World Health Organization has reported that ischemic heart disease (IHD) is the world's largest cause of mortality, resulting in 8.76 million deaths worldwide in 2015 [51]. IHD is caused by a lack of coronary blood supply to the heart, usually because of thrombosis or other acute alterations of coronary atherosclerotic plaques [4]. During myocardial ischemia, characteristic patterns of metabolic and ultrastructural changes lead to irreversible injury. Early restoration of blood flow to the ischemic myocardium is a general treatment strategy for limiting infarct size and reducing mortality caused by IHD [44]. However, the return of blood flow can cause additional cardiac damage and complications and, in many cases, increase infarct size, a situation referred to as myocardial ischemia–reperfusion (I–R) injury

[17]. Myocardial I–R injury is a major contributor to the worldwide morbidity and mortality associated with coronary artery disease [38].

In recent years, an increased awareness of the pathophysiologic mechanisms contributing to myocardial I–R injury has highlighted molecular targets [1, 22]. The inflammatory response not only results in cardiomyocyte apoptosis but also compromises myocardial function. Limiting the extent of myocardial inflammation after myocardial I–R may not only lower mortality, but also help to prevent ventricular arrhythmias and myocardial infarction (MI) [16]. Generation of free radicals after restoration of circulation triggers oxidative stress [20, 21]. Several studies have shown that oxidative stress regulates cell signaling involved in types of cellular death in myocardial I–R injury [37]. It is, therefore, critical to know how to reduce inflammation and oxidative stress to improve the prognosis of patients after myocardial I–R injury.

Growth differentiation factor 11 (GDF11, also known as BMP11), a member of the transforming growth factor beta (TGF- $\beta$ ) superfamily, is broadly expressed throughout tissue [32]. GDF11 levels decline during aging and insufficient GDF11 contributes to age-related cardiac hypertrophy in mice [32]. Long-term targeted myocardial delivery of GDF11 mRNA or daily intraperitoneal injection of protein rejuvenates the heart and enhances chronic cardiac function and cellular regeneration after I–R injury in aged mice [15]. However, the effects of exogenous GDF11 on acute myocardial I–R injury have not previously been reported. In this study, we created myocardial I–R injury by ligating the left anterior descending coronary artery (LAD) in rats for 30 min and then subjected them to 3 h of reperfusion. We hypothesized that treatment with exogenous recombinant GDF11 would reduce myocardial injury and improve myocardial function during acute I–R injury, and enable us to systematically investigate its cardioprotective mechanisms. We also hypothesized that the cardioprotective effects of GDF11 would be antagonized by pretreatment with follistatin (FST), which binds with and neutralizes members of the TGF- $\beta$  superfamily including GDF11.

## Materials and methods

### Animal model

Sprague–Dawley rats (LASCO Co., Charles River Technology, Taipei, Taiwan) weighing 250–300 g were used in this study and cared for according to the advice published in the US National Institutes of Health *Guide for the Care and Use of Laboratory Animals* (NIH Publication No. 85–23, revised 2011). All animals were housed in the Animal Center of Chung Shan Medical University at an ambient

temperature of  $24 \pm 1$  °C and humidity of  $55 \pm 5\%$ , under a 12-h light–dark cycle. The animals were fed normal chow and given water ad libitum. We followed all practical guidelines relating to the surgical procedures and experimental design [3, 31]. The surgical procedures for myocardial I–R injury were reviewed and approved by the Institutional Animal Care and Use Committees of Chung Shan Medical University (IACUC 1855) and Cheng Hsin General Hospital (CHIACUC 104-21).

### Experimental groups

The rats were randomly divided into sham and myocardial I–R groups. Sham-treated animals were treated with 0.1% bovine serum albumin in PBS (0.1% BSA–PBS) without undergoing myocardial I–R injury. In the myocardial I–R group, animals were treated with vehicle (0.1% BSA–PBS) or GDF11 (PEPROTEC, NJ, USA) via the jugular vein 15 min prior to LAD ligation or 10 min prior to reperfusion. GDF11 was administered at a dosage of 0.1 mg/kg, as based on a previous study [32]. Animals in the FST + GDF11 group were administered FST (5  $\mu$ g/kg; PEPROTEC, NJ, USA) 15 min prior to GDF11 administration, following previously described dosage details [30]. Myocardial I–R injury was induced by LAD ligation for 30 min followed by reperfusion for 3 h (Fig. S1). At the end of the experiment, rat hearts or plasma was harvested to observe the effects of GDF11 by triphenyl tetrazolium chloride (TTC) staining, immunoblotting, zymography, ELISA assay, immunohistochemistry, and malondialdehyde (MDA) detection.

### LAD occlusion and reperfusion

Myocardial I–R injury was induced by temporary occlusion of LAD, as previously described [45]. Briefly, the rats were anesthetized with urethane (1.25 g/kg intraperitoneal [i.p.]) then placed on controlled heating pads (TC-1000 Temperature Controller, CWE Inc., USA) with the core temperature measured via a rectal probe maintained at 37 °C. Polyethylene catheters (PE-50) were inserted into the femoral artery for continuous monitoring of heart rate (HR) and arterial blood pressure (BP). A Millar catheter was inserted into the left ventricular (LV) chamber to continuously monitor the maximal slopes of systolic pressure increments ( $+dP/dt$ ) and diastolic pressure decrements ( $-dP/dt$ ). A standard lead-I ECG tracing was recorded via silver electrodes attached to the extremities. Data were recorded by a Transonic Scisense Pressure Measurement System (SP200, Transonic Scisense Inc, Ontario, Canada) and displayed on a data acquisition unit (MP150) and physiological recorder (BIOPAC Systems, Inc., California, USA). The jugular vein was cannulated to administer drugs.

Following tracheotomy, for maintenance of normal  $P_{O_2}$ ,  $P_{CO_2}$  and pH parameters, the animals were ventilated with room air, using a respirator for small rodents (Model 131, NEMI, USA) at a rate of 60 strokes/min and a stroke volume of 10 mL/kg body weight. The chest was opened by left thoracotomy followed by sectioning of the fourth and fifth ribs, 2 mm to the left of the sternum. The heart was quickly externalized and then inverted. A 6/0 silk ligature was placed around the LAD. The heart was repositioned in the chest and the animal was allowed to recover for 15 min. Animals in which the procedure produced arrhythmia or a sustained decrease in mean arterial BP (MBP) to less than 70 mmHg were not included in the study.

### Morphological analysis

Rats were killed for infarct volume analysis (TTC staining) after 30 min of ischemia and 3 h of reperfusion [45]. Following removal, the heart was perfused with cold saline and the flow rate was adjusted to the appropriate range, approximately 3 mL/min. The LAD was then ligated again, followed by perfusion with Evans Blue dye, which stains the remote myocardium but leaves the area at risk (AAR) unstained. Next, the heart was sectioned by a heart matrix slicer (Jacobowitz Systems, Zivic-Miller Laboratories Inc., Allison Park, PA, USA) into standard transverse slices of 2 mm thicknesses. Slices were placed in vital dye TTC (2%; Sigma) at 37 °C in the dark for 30 min and then immersed in formalin 10% at room temperature for 2 days. After scanning the infarcted tissue slices, we assessed the tissue weights by distinguishing the normal myocardium (blue stained) from the AAR and infarct area shown in white on the TTC staining assay.

### Estimation of myocardial damage

Myocardial cellular damage was estimated by measuring the activity of lactate dehydrogenase (LDH) and leakage of troponin I into plasma. Arterial blood was collected from the carotid catheter at the end of myocardial I–R injury for troponin I and LDH measurements using commercially available assay kits (BioVision, Milpitas, CA, USA, and Sigma, St Louis, MO, USA).

### Evaluation of arrhythmia

We assessed the antiarrhythmic effects of GDF11 during myocardial I–R injury. Prior to and during the ischemia and reperfusion periods, HR, BP and ECG changes were simultaneously recorded on a personal computer with waveform analysis software (AcqKnowledge, Biopac System, Goleta, CA, USA). Ventricular ectopic activity was evaluated according to the diagnostic criteria advocated by

the Lambeth Convention [12]. The ECGs were analyzed to determine the incidence and duration of ventricular tachycardias (VTs) and ventricular fibrillations (VFs) in surviving animals and rats that died. VF duration was recorded up until the time when BP was < 15 mmHg in rats that died with irreversible VF.

### Immunoblotting

Left ventricle samples were homogenized with tissue protein extraction reagent (Thermo, Waltham, MA, USA) containing Protease Inhibitor Cocktail (Sigma-Aldrich, St. Louis, MO, USA). Protein concentrations were quantified using a protein assay dye reagent (Bio-Rad, Hercules, CA, USA), using BSA as the standard. Samples were mixed with an equal volume of loading buffer (62.5 mM Tris, pH 6.8, 10% [v/v] glycerol, 2% SDS, 5% [v/v] 2-mercaptoethanol and 0.05% [w/v] bromophenol blue) and heated to 95 °C for 10 min. The sample mixtures were separated with SDS-PAGE gel and transferred onto polyvinylidene difluoride (PVDF) membranes (GE Healthcare, Chicago, IL, USA), which were then blocked with 1% polyvinylpyrrolidone (PVP) or 5% defatted milk combined with 0.05% Tween® 20 in phosphate buffer solution (PBS) at room temperature for 1.5 h, followed by incubation with primary antibodies at 4 °C overnight. The membranes were washed three times with PBS containing 0.1% Tween 20 (PBST), followed by horseradish peroxidase-conjugated secondary antibodies (1:10,000 dilution) at 37 °C for 1 h. After additional PBST washes, the blots were evaluated using an enhanced chemiluminescent system. Primary antibodies included: anti-caspase-3, anti-LC3, anti-Becn1, anti-iNOS, anti-phospho JNK 1/2, anti-JNK 1/2, anti-phospho ERK 1/2, anti-ERK 1/2, and anti-phospho Smad2/3 (Cell Signaling, Danvers, MA, USA); anti-phospho FOXO3, anti-FOXO3, anti-TGF- $\beta$  and anti- $\beta$ -actin (Novus Biologicals, Littleton, CO, USA); anti-HO-1 (Santa Cruz, Dallas, TX, USA); and anti-COX2 (Cayman Chemical, Ann Arbor, MI, USA). Membrane-enhanced chemiluminescence-based immunodetection was conducted using the appropriate horseradish peroxidase secondary antibody. Band density was quantified using ImageJ software and normalized to the internal control; protein levels are presented as the ratio of protein band densities in the sham, vehicle, or GDF11 treatment groups.

### Gelatin zymography

Enhanced activities of matrix metalloproteinase-2 (MMP-2) and matrix metalloproteinase-9 (MMP-9) in the ischemic myocardium were observed following myocardial I–R injury [11]. We, therefore, examined MMP-2 and MMP-9 activities in the left ventricular homogenate using gelatin zymography, as described previously [6]. In brief, samples were

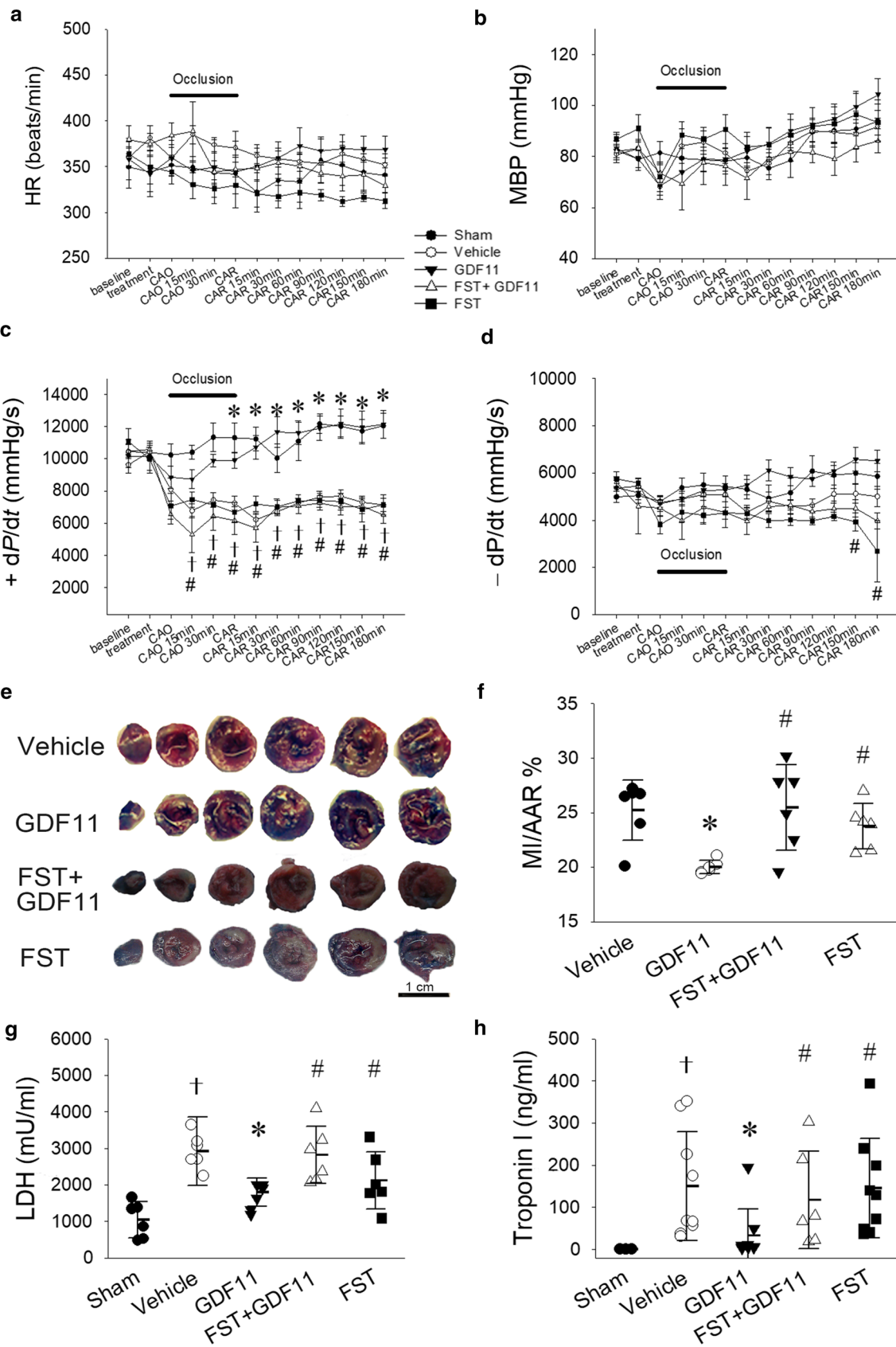


**Fig. 1** GDF11 improved cardiac function and reduced myocardial infarct size during myocardial I–R injury. **a–d** The line graphs show HR and MBP values, as well as  $+dP/dt$  and  $-dP/dt$  changes in left ventricular contractility in sham-operated (closed circles;  $n=7$ ), vehicle-treated (open circles;  $n=7$ ), GDF11-treated (closed triangles;  $n=9$ ) FST+GDF11 (open triangles;  $n=8$ ) and FST-treated (closed squares;  $n=6$ ) animals subjected to myocardial ischemia for 30 min followed by 3 h of reperfusion. Values are expressed as the mean  $\pm$  SEM. **e** Representative photographs of horizontally sliced heart sections are shown: white regions depict infarcted regions; red-stained regions depict ischemic-reperfused but viable regions; blue-stained regions depict non-ischemic regions. **f–h** The MI/AAR % area (ratio of white to red areas), plasma LDH activity and troponin I levels in age-matched animals in the sham-operated group ( $n=6$ ), the vehicle group (controls;  $n=9$ ), the GDF11 group ( $n=9$ ), the FST+GDF11 group ( $n=6$ ) and the FST-only group ( $n=6$ ). Values are expressed as the mean  $\pm$  SD. \* $P<0.05$  compared with vehicle. † $P<0.05$  compared with sham. # $P<0.05$  compared with GDF11. CAOLAD occlusion, CARLAD reperfusion, MI myocardial infarction, AAR area at risk

loaded on 7.5% (w/v) SDS-polyacrylamide gels that had been co-polymerised with 0.1% gelatin (Sigma, St Louis, MO, USA). Stacking gels were 4% (w/v) polyacrylamide and did not contain gelatin substrate. Electrophoresis was performed in running buffer (25 mM Tris, 250 mM glycine, 1% SDS) at room temperature at 125 mA for 1 h. The gel was washed twice at room temperature for 30 min each time in 2.5% Triton X-100, and then washed twice with double-distilled H<sub>2</sub>O for 10 min each time. The gel was incubated in reaction buffer (50 mM Tris, pH 7.5, containing 200 mM NaCl, 10 mM CaCl<sub>2</sub>, 0.02% Brij-35, 0.01% NaN<sub>3</sub>) at 37 °C for 18 h, then stained with 0.25% Coomassie Brilliant Blue R-250 (Sigma, St Louis, MO, USA) for 1 h and destained in 15% methanol/7.5% acetic acid. Gelatinase activity was detected as unstained bands on a blue background. Quantitative analysis of the gelatinolytic enzyme was performed with a computer-assisted imaging densitometer system, UN-SCAN-IT gel Version 6.1 (Silk Scientific, Orem, UT, USA).

### Detection of oxidation stress level

The extent of lipid peroxidation was determined using TBARS Assay Kits (Cayman Chemical, Ann Arbor, MI, USA) measuring total MDA levels. Heart tissues were homogenized in ice-cold PBS then centrifuged at 1600  $\times$ g for 10 min at 4 °C to remove large particles. The MDA–thio-barbituric acid product was formed at 100 °C and quantified colorimetrically at 532 nm.

### TGF- $\beta$ 1 Elisa kits

TGF- $\beta$ 1 concentration in plasma was processed from arterial blood collected from the carotid catheter at the end of myocardial I–R injury and measured using a commercially available assay kits (R&D Systems, Minneapolis, MN, USA).

## In situ detection of apoptosis and MPO-positive immunocytes in myocardium

I–R-damaged myocardium was harvested and embedded in optimal cutting temperature (OCT) compound (Leica, Heidelberg, Germany) and frozen immediately, then sections of 10  $\mu$ m thickness were cut from each tissue block. Terminal deoxynucleotidyl transferase dUTP nick-end labeling (TUNEL) evaluated myocardial apoptosis using the ApopTag Plus Fluorescein In Situ Apoptosis Detection Kits (Millipore, Burlington, MA, USA). Cardiomyocytes were labeled with anti- $\alpha$ -sacromeric actin (Sigma, St Louis, MO, USA). Immunohistochemistry staining identified MPO-positive (MPO<sup>+</sup>) immunocytes in 3- $\mu$ m-thick heart sections fixed in paraformaldehyde, as described previously in methods using anti-MPO (1:50; Spring, Pleasanton, CA, USA) [49]. ProLong<sup>®</sup> Gold Antifade Reagent (Molecular Probes Inc., UK) was used to mount specimens. Images were acquired using a microscope (ZEISS Axio Imager A2) and cell count was quantified with ImageJ<sup>™</sup> software (1.51 v, NIH), as previously described [25].

### Statistical analysis

The effects of drug administration on HR, MBP,  $+dP/dt$  and  $-dP/dt$  values are expressed as the mean  $\pm$  standard error of the mean (SEM) and were assessed using two-way repeated measures ANOVA. The Bonferroni test was used for post hoc pairwise multiple comparisons where necessary. All other data are expressed as the mean  $\pm$  standard deviation (SD). The results are presented with actual data points and were assessed using one-way analysis of variance (ANOVA) or the Kruskal–Wallis test followed by the Student's *t* test, according to the Shapiro–Wilk normality test. Comparisons of the two datasets were performed using the Student's *t* test or Mann–Whitney *U* test. Between-group differences in mortality and incidences of VT and VF were analyzed using the chi-squared test. Statistical significance was defined as  $P<0.05$  in two-tailed testing.

## Results

### Pretreatment with GDF11 improved cardiac function and reduced myocardial infarct size during LAD occlusion and reperfusion

Cardiac function was decreased during LAD occlusion. Treatment with GDF11 did not significantly alter HR or MBP in anesthetized rats during the myocardial I–R period (Fig. 1a, b). We found that  $+dP/dt$  was significantly reduced after LAD occlusion. After myocardial reperfusion,  $+dP/dt$  values in the GDF11-treated group

were significantly higher than those in the vehicle controls (Fig. 1c), whereas  $-dP/dt$  was improved but did not reach significance during 180 min of observation after myocardial I–R. After myocardial I–R injury,  $+dP/dt$  and  $-dP/dt$  were significantly decreased in the FST + GDF11 group compared with rats treated with GDF11 only (Fig. 1c, d). Treatment with FST only did not change cardiac function significantly compared with values in the FST + GDF11 and vehicle-treated groups (Fig. 1c, d). The effects of GDF11 on myocardial I–R-induced mortality and arrhythmias are shown in Table 1. In the vehicle-treated group, I–R-induced mortality was 46%. Administration of GDF11 decreased the mortality rate to 10%, but this did not reach significance ( $P=0.06$ ). Vehicle administration did not elicit arrhythmias in sham-operated rats. VT and VF durations were  $28.6 \pm 8.1$  and  $81.1 \pm 29.9$  s, respectively, in the vehicle-treated group during I–R injury. Administration of GDF11 significantly shortened the durations of VT to  $7.6 \pm 2.7$  s and VF to  $4.9 \pm 2.7$  s, respectively. VT and VF durations were prolonged in animals pretreated with FST alone or in combination with GDF11 compared with values in GDF11-treated animals, but did not differ from VT and VF durations in vehicle-treated animals (Table 1). The effects of GDF11 on myocardial infarct size

are shown in Fig. 1e, f, as well as in Table 2. Evans Blue dye stained the remote myocardium, but not the AAR and infarct area, which are shown in white in the TTC analysis (Fig. 1e). Concordance between the AAR/ventricle % in the vehicle, GDF11, FST + GDF11, and FST-only groups confirmed consistency for the LAD occlusion procedures (Table 2). The infarct size/AAR was significantly reduced in the GDF11-treated group compared with the vehicle-treated group, but was reversed by FST + GDF11 treatment (Fig. 1f). LDH activity and plasma troponin I levels, markers of cellular damage, were both significantly increased in the vehicle-treated group compared with the sham-operated group, but significantly decreased in the GDF11-treated group. Infarct size/AAR % (MI/AAR %), LDH activity and troponin I levels in plasma were significantly increased in the FST + GDF11 group compared with those in the GDF11 group. Pretreatment with FST alone had no significant effects on infarct size or cellular damage (Fig. 1f–h). Hence, administration of GDF11 significantly decreased the impact of myocardial I–R injury, while FST inhibited the cardioprotective effects associated with GDF11 in function and morphology after myocardial I–R injury.

**Table 1** Effects of GDF11 on arrhythmias induced by myocardial I–R (30 min of ischemia and 3 h of reperfusion) in anesthetized rats

	<i>n</i>	Ventricular tachycardia		Ventricular fibrillation		Mortality (%)
		Incidence (%)	Duration (s)	Incidence (%)	Duration (s)	
Sham						
Vehicle	7	–	–	–	–	–
Operated (IR)						
Vehicle	13	85	$28.6 \pm 8.1$	46	$81.1 \pm 29.9$	46
GDF11	10	70	$7.6 \pm 2.7^*$	30	$4.9 \pm 2.7^*$	10
FST + GDF11	15	100 <sup>#</sup>	$75.3 \pm 12.6^{\#}$	53	$53.2 \pm 12.3^{\#}$	40
FST	11	100	$58.32 \pm 18.39^{\#}$	55	$35.23 \pm 15.4$	36

Vehicle = 0.1% BSA–PBS; *n* number of experiments; values for duration of VT and VF are shown as the mean  $\pm$  SEM

\* $P < 0.05$  compared with vehicle

<sup>#</sup> $P < 0.05$  compared with GDF11

**Table 2** Myocardial weight and size of AAR

	Vehicle ( <i>n</i> = 6)	GDF11 ( <i>n</i> = 6)	FST + GDF11 ( <i>n</i> = 6)	FST ( <i>n</i> = 6)
Ventricle weight (g)	$0.84 \pm 0.04$	$0.79 \pm 0.03$	$0.83 \pm 0.02$	$0.81 \pm 0.01$
AAR (g)	$0.57 \pm 0.03$	$0.54 \pm 0.02$	$0.57 \pm 0.01$	$0.56 \pm 0.01$
AAR/Ventricle (%)	$67.97 \pm 0.89$	$68.72 \pm 0.64$	$68.96 \pm 0.27$	$69.68 \pm 0.08$
Infarct size (g)	$0.14 \pm 0.01$	$0.11 \pm 0.01^*$	$0.15 \pm 0.01^{\#}$	$0.13 \pm 0.01^{\#}$

AAR area at risk, Vehicle = 0.1% BSA–PBS; *n* = number of experiments; values are shown as the mean  $\pm$  SEM

\* $P < 0.05$  compared with vehicle

<sup>#</sup> $P < 0.05$  compared with GDF11

## GDF11 reduced apoptosis and deleterious autophagy after myocardial I–R injury

Myocardial I–R injury was associated with programmed cell death, including apoptosis and autophagy. As shown in Fig. 2a, immunoblotting detected caspase-3, LC3, and Beclin-1 expression. The pro- and active (cleaved) forms of caspase-3 were significantly increased in ischemic myocardium after I–R injury in the vehicle-treated group compared with the sham-treated group, while GDF11 treatment was associated with significant reductions in both caspase-3 markers compared with levels in vehicle-treated rats (Fig. 2b). Monitoring of LC3 conversion, LC3 distribution or its flux through the autophagy pathway is widely used to monitor autophagy activity. We found no between-group differences in LC3-I expression amongst the sham-, vehicle-, and GDF11-treated groups, whereas LC3-II and the ratio of LC3-II to LC3-I were significantly decreased in the vehicle- and GDF11-treated groups compared with the sham-treated group (Fig. 2c). In the nucleation step of autophagy, Beclin-1 plays an important role and causes excessive autophagy during reperfusion [33, 45]. Administration of GDF11 significantly decreased Beclin-1 expression 0.46-fold compared with vehicle administration (Fig. 2d). These findings suggest that GDF11 reduces apoptosis and deleterious autophagy in rats after myocardial I–R injury.

## GDF11 decreased inflammation after myocardial I–R injury

MI or I–R injury stimulates the production of inducible nitric oxide synthase (iNOS) and cyclooxygenase 2 (COX2), causing inflammation [49]. Using immunoblotting, we assessed levels of iNOS and COX2 expression (Fig. 3a). In the vehicle-treated group, iNOS and COX2 expression was significantly increased after myocardial I–R injury. Treatment with GDF11 significantly decreased iNOS and COX2 expression by 0.59- and 0.38-fold, respectively. The effects of GDF11 on the activities of MMP-2 and MMP-9 in rats subjected to myocardial I–R injury are shown in Fig. 3b. MMP-2 activity was not altered following vehicle or GDF11 treatment. Notably, MMP-9 activity was dramatically increased in the vehicle-treated group compared to the sham-operated group. Administration of GDF11 significantly reduced MMP-9 activity in the myocardium after I–R injury, while infiltration of MPO-expressing immunocytes into the infarct border was significantly reduced by GDF11 pretreatment compared with vehicle pretreatment (Fig. 3c). Our data show that GDF11 reduces I–R-induced inflammation in the myocardium.

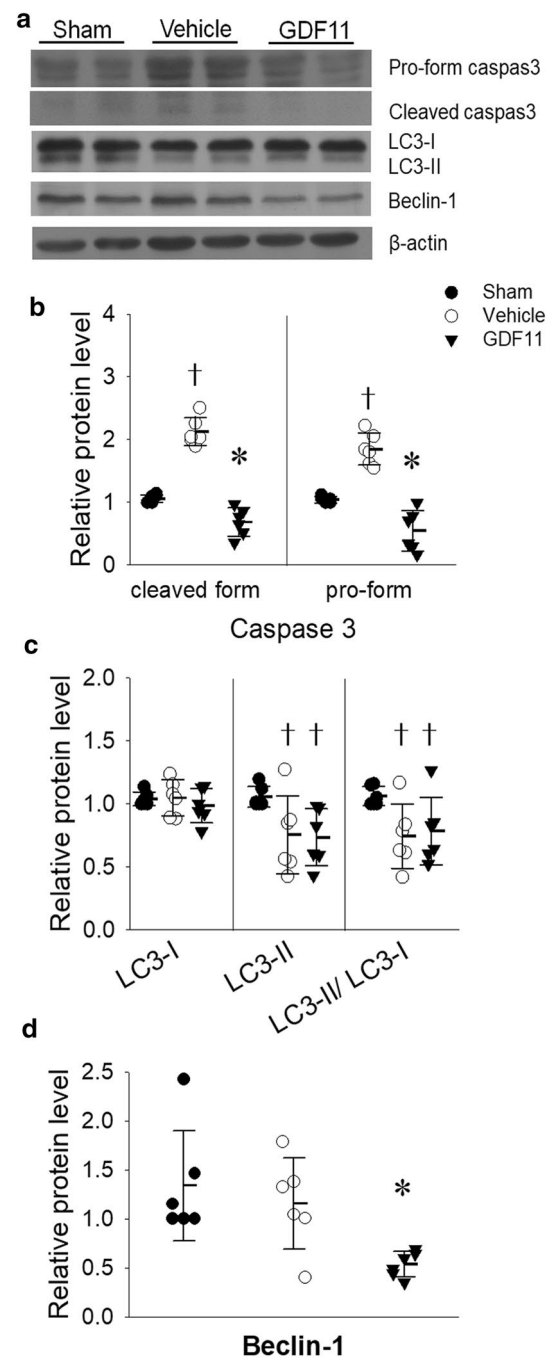


**Fig. 2** GDF11 treatment effectively reduced cellular apoptosis and deleterious autophagy after myocardial I–R injury. **a** Western blot assays display the expression levels of pro-caspase-3, cleaved caspase-3, LC3-I/II, Beclin-1 and  $\beta$ -actin. **b–d** Relative protein levels of cleaved caspase-3, pro-caspase-3, LC3-I/II and Beclin-1, after normalization to  $\beta$ -actin. The results are shown as the mean  $\pm$  SD ( $n=6-8$ ). \* $P < 0.05$  compared with vehicle. † $P < 0.05$  compared with sham

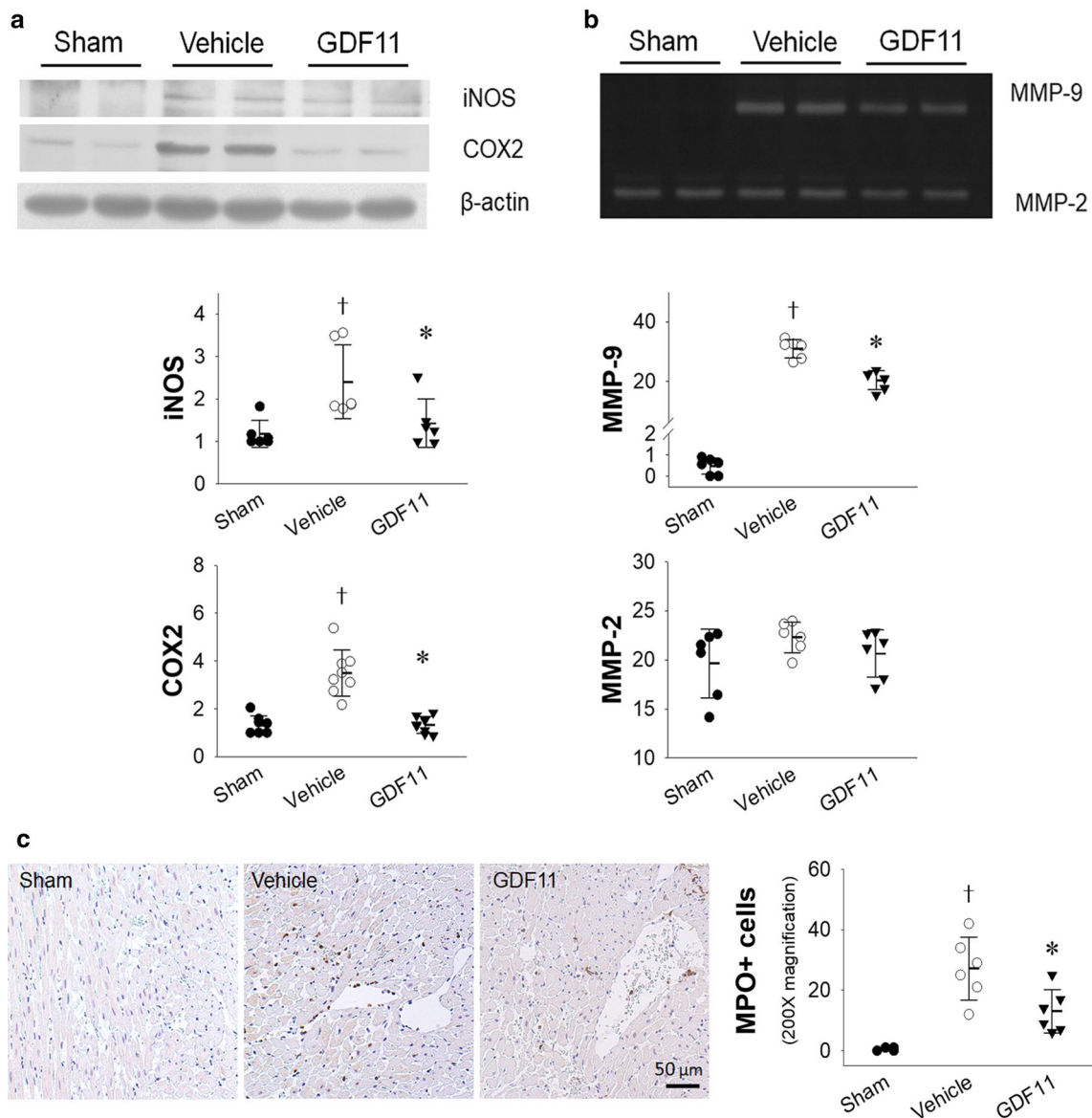


**Fig. 3** GDF11 treatment effectively reduced inflammation after myocardial I-R injury. **a** Western blot results display the expression levels of iNOS, COX2 and  $\beta$ -actin. Relative protein levels of iNOS and COX2 after normalization to  $\beta$ -actin. **b** Gelatin zymography analysis for MMP-2 and MMP-9 activities in rat heart tissue samples after myocardial I-R injury. Values of optical densities in arbitrary units

(A.U.). **c** MPO, a marker of neutrophil and macrophage activation, was stained and quantified. GDF11 inhibits MPO+ cells infiltration in infarcted myocardium. The results are shown as the mean  $\pm$  SD ( $n=6-8$ ). \* $P<0.05$  compared with vehicle. † $P<0.05$  compared with sham

### GDF11 increased heme oxygenase-1 (HO-1) and decreased oxidative stress after myocardial I-R injury

The enzyme HO-1 responds to stress such as oxidative stress and hypoxia. According to in vitro and in vivo evidence, increased HO-1 levels play a protective role against inflammatory damage and oxidative stress in response to I-R injury [48]. In this study, HO-1 expression detected by immunoblotting was significantly increased after 30 min

of ischemia and 3 h of reperfusion (Fig. 4a). HO-1 protein expression in the myocardium after I-R injury was enhanced to a greater extent in GDF11-treated rats compared with vehicle-treated rats. These data indicate that GDF11 escalates HO-1 expression still further after myocardial I-R injury. Heart tissue MDA level was significantly increased after myocardial I-R injury in the vehicle-treated group compared with those in the sham-treated group, while GDF11 pretreatment significantly suppressed MDA levels compared with vehicle treatment (Fig. 4b).

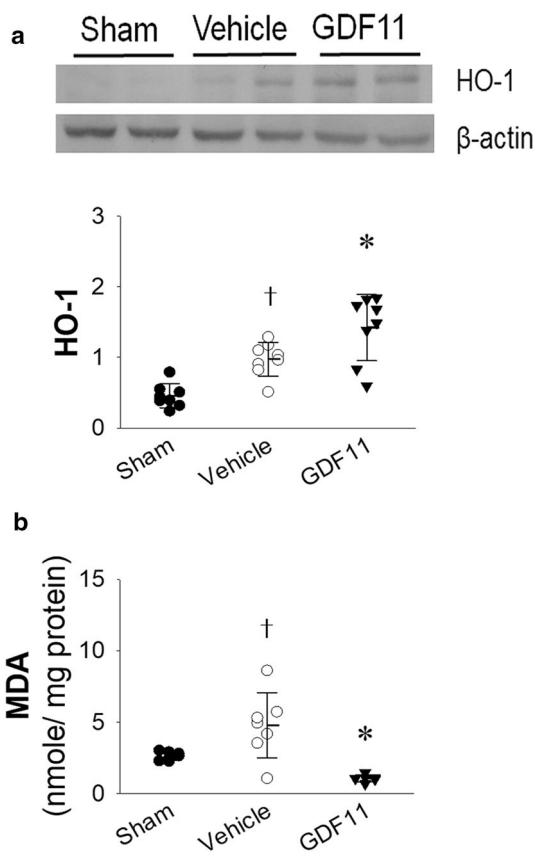


**Fig. 4** Effects of GDF11 on protein expression levels of HO-1 and MDA in rats subjected to myocardial I–R injury. **a** Western blot results depict the expression levels of HO-1. Relative protein levels of HO-1 were quantified after normalization to  $\beta$ -actin. **b** Myocardial oxidative stress markers was evaluated by MDA contents. The results are shown as the mean  $\pm$  SD ( $n=6-8$ ). \* $P < 0.05$  compared with vehicle. † $P < 0.05$  compared with sham

### GDF11 decreased activation of c-JUN N-terminal kinase (JNK) and extracellular signal-regulated kinase (ERK) signaling after myocardial I–R injury

JNK and ERK expression and activity levels were measured by immunoblotting (Fig. 5a). Myocardial I–R led to an increase in JNK1/2 but not ERK1/2 protein expression, which was not significantly altered by GDF11 administration. In contrast, JNK1/2 and ERK1/2 activities were significantly increased in I–R-injured animals compared with sham-operated animals. GDF11 significantly suppressed the increases in phospho (p)-JNK1/2 and p-ERK1/2 seen after vehicle administration (Fig. 5b). FST pretreatment blocked the effects of GDF11 on JNK1/2 and ERK1/2 activation (Fig. S2). Notably, GDF11 significantly reduced JNK and ERK activities in the myocardium after I–R injury.

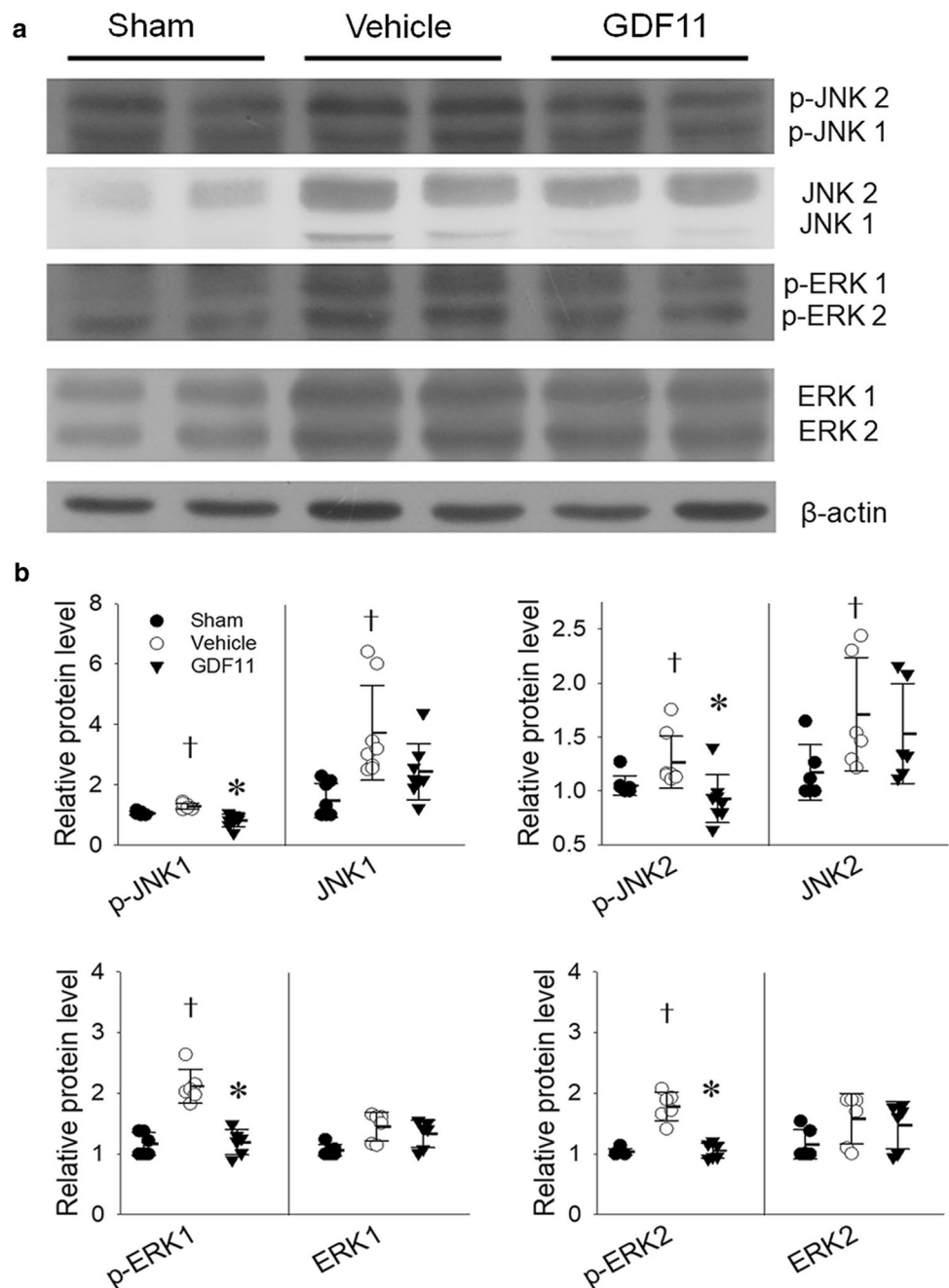
### GDF11 increased the activation of Smad2/3 but not transcription factor forkhead box O3 (FOXO3) after myocardial I–R injury

It is speculated that intracellular FOXO3 and Smad2/3 signaling may play an important role in the cardioprotection associated with GDF11 in myocardial I–R injury [52]. FOXO3 has been found to be a critical physiological regulator of oxidative stress in mammalian cells [34]. However, in this study, we found no significant between-group differences in levels of phosphorylated FOXO3 (p-FOXO3), FOXO3, or the ratio of phospho to total FOXO3 among sham-operated, vehicle- and GDF11-treated groups. The active form of FOXO3 (unphosphorylated FOXO) was reduced in the FST + GDF11 group (Fig. 6a). Binding of the activin type 2 receptor induces the recruitment and phosphorylation of an activin type 1 receptor, which then phosphorylates the intracellular signaling proteins Smad2 and Smad3 [42]. In this study, after myocardial I–R injury, we found that phospho (p)-Smad2 and p-Smad3 levels did not differ significantly between the vehicle-treated and sham-operated groups, whereas GDF11 administration was associated with significant increases in p-Smad2 and combined p-Smad2 and p-Smad3 (p-Smad2/3) expression. We observed significant reductions in levels of p-Smad2 and p-Smad2/3 expression in the FST + GDF11-treated group compared with the GDF11-treated group and we noted an increasing trend in p-Smad3 expression, which failed to reach significance (Fig. 6b). Our data suggest that GDF11 activates Smad2/3, the typical pathway of the TGF- $\beta$  superfamily, but not FOXO3, in I–R-injured myocardium.

### GDF11 decreased plasma TGF- $\beta$ levels after myocardial I–R injury

Protein levels of TGF- $\beta$  are reportedly increased in acute MI [7, 13]. To clarify whether Smad2/3 was activated by TGF- $\beta$  or GDF11, we analyzed plasma TGF- $\beta$  concentrations (Fig. 6c). After myocardial I–R, TGF- $\beta$  levels were increased in vehicle-treated animals compared to those in sham-operated animals, while a significant decrease in TGF- $\beta$  levels associated with GDF11 treatment was reversed by FST pretreatment. To determine the effects of GDF11 on TGF- $\beta$  expression, we used western blot to analyze TGF- $\beta$  levels in myocardial tissue (Fig. S3). Levels of unprocessed and mature TGF- $\beta$  were significantly increased after myocardial I–R injury. Pretreatment with FST enhanced TGF- $\beta$  synthesis in myocardium, whereas GDF11 did not affect the translation and maturation of TGF- $\beta$  compared to vehicle treatment. These experiments show that GDF11 suppresses mature TGF- $\beta$  secretion in rats following myocardium I–R injury.

**Fig. 5** GDF11 suppressed TGF- $\beta$  and the non-canonical pathway, ERK and JNK, in rats subjected to myocardial I–R injury. **a** Western blot results display the expression and phosphorylation levels of ERK1, ERK2, JNK1, and JNK2.  $\beta$ -actin was used as the internal control. **b** Relative protein levels of p-JNK1/2, JNK1/2, p-ERK1/2 and ERK1/2 were quantified after normalization to  $\beta$ -actin. The results are shown as the mean  $\pm$  SD ( $n=6-8$ ). \* $P<0.05$  compared with vehicle. † $P<0.05$  compared with sham



### Post-ischemic treatment with GDF11 improved cardiac function and reduced myocardial damage

To simulate clinical treatment in acute MI, GDF11 was administered 10 min before restoration of blood flow. HR and MBP were not significantly altered in anesthetized rats during the myocardial I–R period (Fig. S4). We found that  $+dP/dt$  values were significantly improved after GDF11 treatment compared to values in vehicle controls (Fig. 7a). We also observed elevations in  $-dP/dt$  at the end of ischemia (CAO 30 min) and again at 30 min after reperfusion (CAR

30–180 min) (Fig. 7b). Post-ischemic treatment with GDF11 demonstrated a dramatic effect on cardiac function after reperfusion damage.

The effects of post-treatment GDF11 on myocardial infarct size are shown in Fig. 7c. Significant reductions in MI/AAR %, as well as in plasma troponin I levels, were observed in the GDF11-treated animals compared with the vehicle-treated animals, although there was no between-group difference in LDH activity ( $1908.5 \pm 325.5$   $\mu$ L vs  $1255.8 \pm 272.0$   $\mu$ L, respectively). The TUNEL assay revealed a substantial reduction in apoptotic DNA

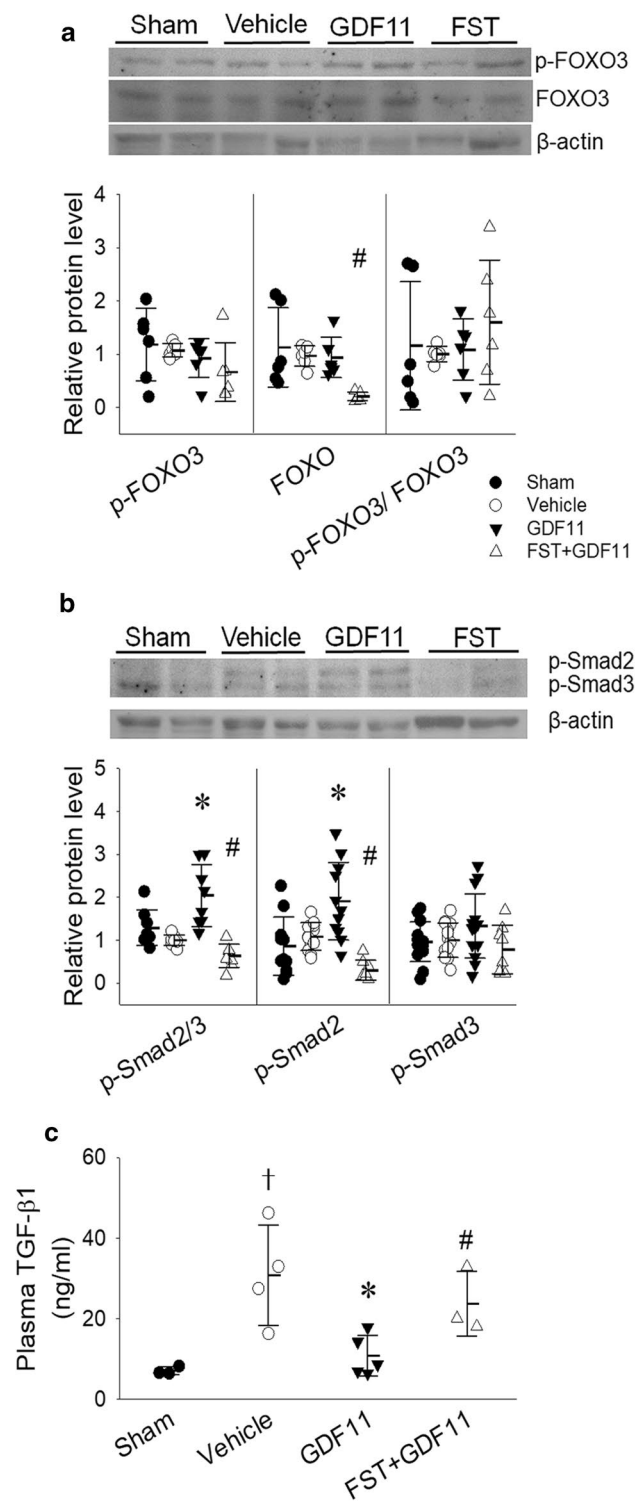


**Fig. 6** GDF11 did not regulate FOXO3, but enhanced Smad 2/3 signaling and decreased TGF-β secretion in rats subjected to myocardial I-R injury. **a**, **b** Western blot results depict expression levels of FOXO3 and p-FOXO3, and p-Smad2/3. β-actin was used as the internal control. **c** TGF-β cytokine levels in plasma from rats after myocardial I-R, as measured by ELISA. The results are presented as the mean ± SD ( $n=6-12$  for western blot, and  $n=3-5$  for ELISA). \* $P<0.05$  compared with vehicle. † $P<0.05$  compared with sham. # $P<0.05$  compared with GDF11

fragmentation in the GDF11-treated animals, and GDF11 also markedly suppressed the infiltration of MPO-positive immunocytes into the infarct border (Fig. 7g, h). A reduction in MDA levels demonstrated a significant attenuation of oxidative stress in hearts of rats treated with GDF11 before reperfusion (Fig. 7f). Hence, administration of GDF11 before reperfusion restored blood flow after ischemia, indicating that it protects ischemic myocardium against reperfusion injury.

### Discussion

This is the first study to demonstrate the cardioprotective effects of GDF11 in rats subjected to acute myocardial I-R injury. Administration of GDF11 significantly improved cardiac function and MI but did not alter MBP or HR during 30 min of myocardial ischemia and 3 h of reperfusion. The cardioprotective effects of GDF11 were associated with marked attenuations in myocardial inflammation and oxidative stress. Moreover, inflammatory effects, as assessed by levels of iNOS, COX2 and MPO expression, were reduced and MMP-9 was inhibited after GDF11 treatment. GDF11 suppressed ERK and JNK activation as well as inflammation in the myocardium after I-R injury. We also found that GDF11 enhanced the expression of HO-1 (a key factor for antioxidation) in the infarcted myocardium. Oxidative damage was also decreased in GDF11-treated hearts. We found that GDF11 activated the Smad2/3 complex, but suppressed TGF-β levels in the circulation. Pretreatment with the GDF11 inhibitor, FST, prevented the beneficial effects of GDF11 and blocked the activation of Smad2/3 signaling in rats subjected to myocardial I-R injury. These results indicate that GDF11 may protect the myocardium and improve cardiac function after I-R injury via anti-inflammatory and antioxidative effects.

GDF11 is a member of the activin subfamily, which is also classified as a member of the TGF-β superfamily, capable of activating the Smad2/3 signaling pathway via binding to the TGF-β type I and II receptors [30]. GDF11 appears to preserve the regenerative ability of stem cells [47]. Recent research has also reported that long-term targeted myocardial delivery of GDF11 mRNA or protein rejuvenates the aged (21-month-old) mouse heart and enhances chronic cardiac function and cellular regeneration after I-R injury [15]. The evidence from these studies demonstrates that GDF11 can enhance cellular self-protection or repair and thereby protect organs against not only aging but also I-R injury. In contrast, other research has reported that daily injections of biologically active GDF11 raised the levels of GDF11 in aged mice blood, but had no effects upon the heart, including cardiomyocyte size, cardiac structure, or cardiac function [47]. In addition, long-term GDF11 administration in cell-based

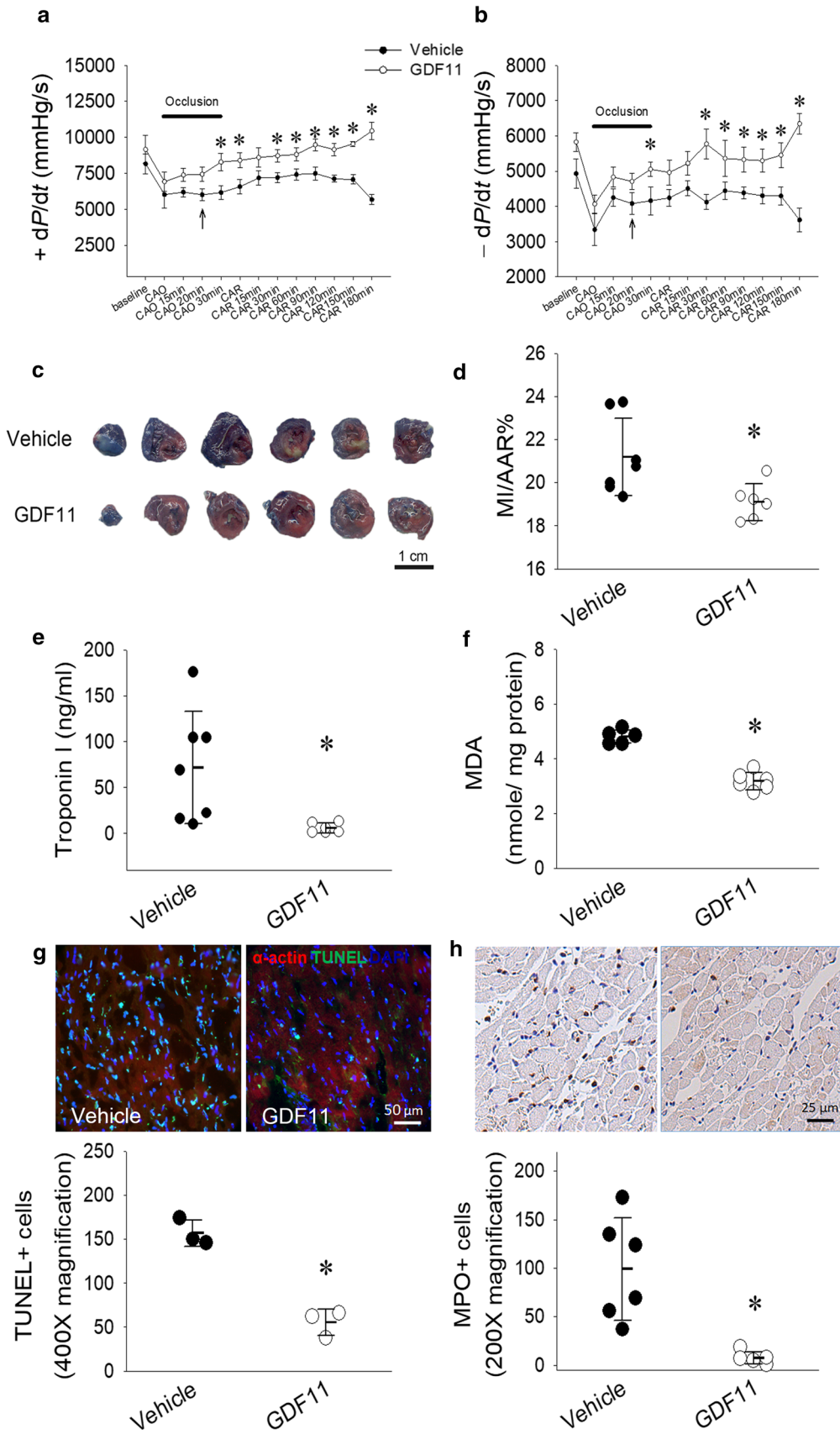


**Fig. 7** Treatment with GDF11 after ischemia and prior to reperfusion improved cardiac function and reduced myocardial damage. **a, b** Line graphs show  $+dP/dt$  and  $-dP/dt$  changes in left ventricular contractility in vehicle-treated (closed circles;  $n=6$ ) and GDF11-treated (open triangles;  $n=6$ ) animals subjected to myocardial ischemia for 30 min followed by 3 h of reperfusion. The arrows indicate time points of GDF11 or vehicle administration given via the jugular veins. Values are expressed as the mean  $\pm$  SEM. **c** Representative photographs of horizontally sliced heart sections are shown: white regions depict infarcted regions; red-stained regions depict ischemic-reperfused but viable regions; blue-stained regions depict non-ischemic regions. The MI/AAR % area (ratio of white to red areas) and troponin I levels in age-matched animals in the vehicle group (controls;  $n=7$ ) and GDF11 group ( $n=6$ ). **d, e** GDF11 inhibits apoptosis and MPO+ cell infiltration in infarcted myocardium. Apoptotic nuclei were labeled by TUNEL (green), and then counterstained to mark nuclei (DAPI, blue) and cardiomyocytes ( $\alpha$ -actin, red). MPO, a marker of neutrophil and macrophage activation, was stained and quantified ( $n=6$ ). **f** MDA content suggested that treatment with GDF11 reduces oxidative stress ( $n=6$ ). Values are expressed as the mean  $\pm$  SD. \* $P < 0.05$  compared with vehicle. CAOLAD occlusion, CARLAD reperfusion, MI myocardial infarction, AAR area at risk

and animal studies was associated with the suppression of erythrocyte maturation and symptoms of cachexia in recent research [19, 42]. We speculate that although the effects of GDF11 remain uncertain in aging cardiac tissue or tissue reflecting long-term myocardial injury, GDF11 may help to protect the myocardium during the acute phase of I–R injury.

A key strategy for rescuing the penumbra after I–R injury is to reduce cell death. It is well established that programmed cell death, including apoptosis and autophagy, is upregulated in myocardial I–R [26]. A death-inducing signaling complex activates the caspase cascade, which in turn cleaves and activates caspase-3, an executioner caspase that proteolyzes many cellular proteins [26, 50]. Autophagy plays a pivotal role in maintaining metabolism in cells subjected to stressful conditions [41]. However, severe oxidative damage induces overactivation of autophagy during reperfusion, resulting in excessive cell death [40]. Reactive oxygen species (ROS) modulate autophagy by fine-tuning transcription factor activity, inducing the expression of autophagic genes such as *Beclin 1* [8, 14, 18]. Other researchers have reported that the activation of Beclin-1 leads to excessive autophagy during the reperfusion phase; nevertheless, the induction of autophagy and cardiac injury were significantly attenuated in *beclin 1*<sup>+/-</sup> mice [35]. In our study, expression levels of cleaved caspase-3 and Beclin-1 were reduced in GDF11-treated rats, although GDF11 was not associated with any recovery in the downregulation of the autophagic marker, LC3II, after myocardial I–R injury. These data suggest that GDF11 suppresses apoptosis and detrimental autophagy in I–R-injured rats.

Inflammation is the hallmark of myocardial I–R injury. Several studies report that iNOS is induced in ischemic myocardium and that inhibition of iNOS can reduce MI [29]. iNOS is the enzyme responsible for NO production

by proinflammatory M1 macrophages [10]. Previous studies have demonstrated that myocardial I–R injury increases COX2 activation in the myocardium and that treatment with a COX2 inhibitor can decrease infarct size and ameliorate cardiac function [43]. In the acute stage of MI, increased MMP activity degrades the pre-existing extracellular membrane (ECM) and enhances the migration of inflammatory cells into the infarcted zone to remove necrotic myocytes [39]. MPO, a highly copious enzyme in neutrophils and inflammatory monocytes, is capable of triggering oxidative damage. MPO inhibitors show protective effects in acute and chronic MI. In our study, administration of GDF11 reduced iNOS, COX2, and MMP9 expression, as well as MPO-expressing immunocyte infiltration into the infarct border. Our data demonstrate anti-inflammatory effects associated with GDF11 that protect the heart against myocardial I–R injury.

Antioxidant, anti-inflammatory and anti-apoptotic effects of the inducible enzyme HO-1 are induced during I–R injury [2]. Smad signaling and specificity protein 1 (Sp1) are both required for TGF- $\beta$ 1 to induce human HO-1 promoter–reporter activity. Overexpression of Smad2, Smad3 and Smad4 has been shown to increase HO-1 promoter basal activity [46]. HO-1 increased post-ischemic blood flow, diminished inflammation, and improved myocyte regenerative potential in an ischemic limb model [24]. It is also known that HO-1 expression is regulated by ERK [23]. In this study, we found that HO-1 and MDA increased after I–R injury and that GDF11 enhanced Smad2/3 activation and promoted HO-1 expression, which reduced myocardial oxidative stress. We speculate that HO-1 plays an important role in the cardioprotective effects of GDF11 in the acute stage of myocardial I–R.

TGF- $\beta$  and other members of the TGF- $\beta$  superfamily bind to their corresponding receptors, such as ALK5, and thereby constitute multifunctional signaling pathways that regulate the Smad (canonical) signaling pathway and non-canonical pathway. Positive regulation of TGF- $\beta$  could occur through the actions of TGF- $\beta$ -like factors [36]. Hence, we speculated that exogenous GDF11 might serve as a partial agonist that interferes with the activation of the TGF receptor. Earlier research assumed that the FOXO3 pathway is suppressed by GDF11 and plays a key role in the mechanism of GDF11 against I–R injury [52]. In the non-canonical pathway, MAPK signaling is activated by TGF- $\beta$  via the ALK5 receptor, which has been shown to regulate many physical and pathological effects [5]. In our study, we discovered that circulating TGF- $\beta$  concentrations were decreased after GDF11 treatment; GDF11 activated Smad2/3 without influencing the FOXO3 pathway, and also suppressed JNK and ERK activation. Our data support the contention that exogenous GDF11 reduces the downstream signaling of TGF- $\beta$  through the non-canonical

pathway during myocardial I–R injury. We, therefore, speculate that GDF11 downregulates TGF- $\beta$  signaling, but not that of the canonical Smad signaling pathway, during the acute stage of myocardial I–R.

FST has previously been used to inhibit the action of GDF11 [28]. We found that pretreatment with FST prevented the beneficial effects of GDF11 in rats subjected to myocardial I–R injury. However, as FST is not a specific inhibitor of GDF11, it could also block other members of the activin family. Hence, FST administration might explain the reduction in the expression of FOXO (Fig. 6a) and elevation in TGF- $\beta$  expression in the myocardium (Fig. S3). One previous study has reported that FST at the dose of 10  $\mu$ g per mouse reduces myocardial I–R injury [9]. The dosage of FST used in our study (5  $\mu$ g/kg) is almost 80-fold lower than that used in preclinical cardioprotective investigations. We found in our study that FST alone was not associated with any cardioprotective advantages or disadvantages.

Although reperfusion therapy is the major therapeutic strategy for MI, this approach is associated with elevations in inflammation and oxidative stress [27]. Previous research has shown that long-term expression of GDF11 in the myocardium after reperfusion increases cardiac stem cell proliferation and reduces cell senescence [15]. In our study, administration of GDF11 at 10 min prior to reperfusion significantly prevented cardiac dysfunction after myocardial I–R injury. Furthermore, we observed that GDF11 reduced the levels of inflammation and oxidative stress caused by myocardial reperfusion injury.

In conclusion, our results highlight the finding that exogenous recombinant GDF11 contributes to morphologic and functional recovery after myocardial I–R injury. GDF11 reduces inflammation and oxidation during the acute stage of myocardial I–R. This research indicates that the beneficial effects of GDF11 are exerted during the early stage of myocardial I–R injury. According to our evidence, GDF11 shows potential as a novel therapy for restoring heart function after I–R insult.

**Acknowledgements** Cryostat preparation for frozen sections and upright fluorescence microscopy investigations were performed in the Instrument Center of Chung Shan Medical University, which is supported by Chung Shan Medical University and National Science Council, Ministry of Education, Taichung, Taiwan.

**Funding** This work was supported by research grants from Taiwan's Ministry of Science and Technology (MOST) 106-2320-B-040-005 and MOST 106-2314-B-350-003 given to S-SH and S-KT.

### Compliance with ethical standards

**Conflicts of interest** All authors declare that they have no conflicts of interest.

## References

1. Arumugam TV, Okun E, Tang SC, Thundyil J, Taylor SM, Woodruff TM (2009) Toll-like receptors in ischemia-reperfusion injury. *Shock* 32:4–16. <https://doi.org/10.1097/SHK.0b013e318193e333>
2. Bolisetty S, Zarjou A, Agarwal A (2017) Heme oxygenase 1 as a therapeutic target in acute kidney injury. *Am J Kidney Dis* 69:531–545. <https://doi.org/10.1053/j.ajkd.2016.10.037>
3. Botker HE, Hausenloy D, Andreadou I, Antonucci S, Boengler K, Davidson SM, Deshwal S, Devaux Y, Di Lisa F, Di Sante M, Efentakis P, Femmino S, Garcia-Dorado D, Giricz Z, Ibanez B, Iliodromitis E, Kaludercic N, Kleinbongard P, Neuhauser M, Ovize M, Pagliaro P, Rahbek-Schmidt M, Ruiz-Meana M, Schluter KD, Schulz R, Skyschally A, Wilder C, Yellon DM, Ferdinandy P, Heusch G (2018) Practical guidelines for rigor and reproducibility in preclinical and clinical studies on cardioprotection. *Basic Res Cardiol* 113:39. <https://doi.org/10.1007/s00395-018-0696-8>
4. Buja LM (2005) Myocardial ischemia and reperfusion injury. *Cardiovasc Pathol* 14:170–175. <https://doi.org/10.1016/j.carpath.2005.03.006>
5. Cargnello M, Roux PP (2011) Activation and function of the MAPKs and their substrates, the MAPK-activated protein kinases. *Microbiol Mol Biol Rev* 75:50–83. <https://doi.org/10.1128/MMBR.00031-10>
6. Chen KM, Lee HH, Lu KH, Tseng YK, Hsu LS, Chou HL, Lai SC (2004) Association of matrix metalloproteinase-9 and Purkinje cell degeneration in mouse cerebellum caused by *Angiostromylylus cantonensis*. *Int J Parasitol* 34:1147–1156. <https://doi.org/10.1016/j.ijpara.2004.07.004>
7. Chen LL, Yin H, Huang J (2007) Inhibition of TGF-beta1 signaling by eNOS gene transfer improves ventricular remodeling after myocardial infarction through angiogenesis and reduction of apoptosis. *Cardiovasc Pathol* 16:221–230. <https://doi.org/10.1016/j.carpath.2007.02.007>
8. Chen Y, McMillan-Ward E, Kong J, Israels SJ, Gibson SB (2008) Oxidative stress induces autophagic cell death independent of apoptosis in transformed and cancer cells. *Cell Death Differ* 15:171–182. <https://doi.org/10.1038/sj.cdd.4402233>
9. Chen Y, Rothnie C, Spring D, Verrier E, Venardos K, Kaye D, Phillips DJ, Hedger MP, Smith JA (2014) Regulation and actions of activin A and follistatin in myocardial ischaemia-reperfusion injury. *Cytokine* 69:255–262. <https://doi.org/10.1016/j.cyto.2014.06.017>
10. Choo EH, Lee JH, Park EH, Park HE, Jung NC, Kim TH, Koh YS, Kim E, Seung KB, Park C, Hong KS, Kang K, Song JY, Seo HG, Lim DS, Chang K (2017) Infarcted myocardium-primed dendritic cells improve remodeling and cardiac function after myocardial infarction by modulating the regulatory T cell and macrophage polarization. *Circulation* 135:1444–1457. <https://doi.org/10.1161/CIRCULATIONAHA.116.023106>
11. Chow AK, Cena J, Schulz R (2007) Acute actions and novel targets of matrix metalloproteinases in the heart and vasculature. *Br J Pharmacol* 152:189–205. <https://doi.org/10.1038/sj.bjp.0707344>
12. Curtis MJ, Hancox JC, Farkas A, Wainwright CL, Stables CL, Saint DA, Clements-Jewery H, Lambiase PD, Billman GE, Janse MJ, Pugsley MK, Ng GA, Roden DM, Camm AJ, Walker MJ (2013) The Lambeth conventions (II): guidelines for the study of animal and human ventricular and supraventricular arrhythmias. *Pharmacol Ther* 139:213–248. <https://doi.org/10.1016/j.pharmthera.2013.04.008>
13. Deten A, Holz A, Leicht M, Barth W, Zimmer HG (2001) Changes in extracellular matrix and in transforming growth factor beta isoforms after coronary artery ligation in rats. *J Mol Cell Cardiol* 33:1191–1207. <https://doi.org/10.1006/jmcc.2001.1383>

14. Djavaheri-Mergny M, Amelotti M, Mathieu J, Besancon F, Bauvy C, Souquere S, Pierron G, Codogno P (2006) NF-kappaB activation represses tumor necrosis factor-alpha-induced autophagy. *J Biol Chem* 281:30373–30382. <https://doi.org/10.1074/jbc.M602097200>
15. Du GQ, Shao ZB, Wu J, Yin WJ, Li SH, Wu J, Weisel RD, Tian JW, Li RK (2017) Targeted myocardial delivery of GDF11 gene rejuvenates the aged mouse heart and enhances myocardial regeneration after ischemia-reperfusion injury. *Basic Res Cardiol* 112:7. <https://doi.org/10.1007/s00395-016-0593-y>
16. Eltzschig HK, Eckle T (2011) Ischemia and reperfusion—from mechanism to translation. *Nat Med* 17:1391–1401. <https://doi.org/10.1038/nm.2507>
17. Folino A, Losano G, Rastaldo R (2013) Balance of nitric oxide and reactive oxygen species in myocardial reperfusion injury and protection. *J Cardiovasc Pharmacol* 62:567–575. <https://doi.org/10.1097/FJC.0b013e3182a50c45>
18. Hariharan N, Zhai P, Sadoshima J (2011) Oxidative stress stimulates autophagic flux during ischemia/reperfusion. *Antioxid Redox Signal* 14:2179–2190. <https://doi.org/10.1089/ars.2010.3488>
19. Harper SC, Johnson J, Borghetti G, Zhao H, Wang T, Wallner M, Kubo H, Feldsott EA, Yang Y, Joo Y, Gou X, Sabri AK, Gupta P, Myzithras M, Khalil A, Franti M, Houser SR (2018) GDF11 decreases pressure overload-induced hypertrophy, but can cause severe cachexia and premature death. *Circ Res* 123:1220–1231. <https://doi.org/10.1161/CIRCRESAHA.118.312955>
20. Hashemi M (2014) The study of pentoxifylline drug effects on renal apoptosis and BCL-2 gene expression changes following ischemic reperfusion injury in rat. *Iran J Pharm Res* 13:181–189
21. Hausenloy DJ, Botker HE, Engstrom T, Erlinge D, Heusch G, Ibanez B, Kloner RA, Ovize M, Yellon DM, Garcia-Dorado D (2017) Targeting reperfusion injury in patients with ST-segment elevation myocardial infarction: trials and tribulations. *Eur Heart J* 38:935–941. <https://doi.org/10.1093/eurheartj/ehw145>
22. Heusch G, Gersh BJ (2017) The pathophysiology of acute myocardial infarction and strategies of protection beyond reperfusion: a continual challenge. *Eur Heart J* 38:774–784. <https://doi.org/10.1093/eurheartj/ehw224>
23. Iles KE, Dickinson DA, Wigley AF, Welty NE, Blank V, Forman HJ (2005) HNE increases HO-1 through activation of the ERK pathway in pulmonary epithelial cells. *Free Radic Biol Med* 39:355–364. <https://doi.org/10.1016/j.freeradbiomed.2005.03.026>
24. Jazwa A, Stoszko M, Tomczyk M, Bukowska-Strakova K, Pichon C, Jozkowicz A, Dulak J (2015) HIF-regulated HO-1 gene transfer improves the post-ischemic limb recovery and diminishes TLR-triggered immune responses—effects modified by concomitant VEGF overexpression. *Vascul Pharmacol* 71:127–138. <https://doi.org/10.1016/j.vph.2015.02.011>
25. Jensen EC (2013) Quantitative analysis of histological staining and fluorescence using ImageJ. *Anat Rec (Hoboken)* 296:378–381. <https://doi.org/10.1002/ar.22641>
26. Kalogeris T, Baines CP, Krenz M, Korthuis RJ (2012) Cell biology of ischemia/reperfusion injury. *Int Rev Cell Mol Biol* 298:229–317. <https://doi.org/10.1016/b978-0-12-394309-5.00006-7>
27. Kalogeris T, Bao Y, Korthuis RJ (2014) Mitochondrial reactive oxygen species: a double edged sword in ischemia/reperfusion vs preconditioning. *Redox Biol* 2:702–714. <https://doi.org/10.1016/j.redox.2014.05.006>
28. Khalil AM, Dotimas H, Kahn J, Lamerdin JE, Hayes DB, Gupta P, Franti M (2016) Differential binding activity of TGF-beta family proteins to select TGF-beta receptors. *J Pharmacol Exp Ther* 358:423–430. <https://doi.org/10.1124/jpet.116.232322>
29. Li Q, Guo Y, Tan W, Stein AB, Dawn B, Wu WJ, Zhu X, Lu X, Xu X, Siddiqui T, Tiwari S, Bolli R (2006) Gene therapy with iNOS provides long-term protection against myocardial infarction without adverse functional consequences. *Am J Physiol Heart Circ Physiol* 290:H584–H589. <https://doi.org/10.1152/ajpheart.00855.2005>
30. Li S, Nie EH, Yin Y, Benowitz LI, Tung S, Vinters HV, Bahjat FR, Stenzel-Poore MP, Kawaguchi R, Coppola G, Carmichael ST (2015) GDF10 is a signal for axonal sprouting and functional recovery after stroke. *Nat Neurosci* 18:1737–1745. <https://doi.org/10.1038/nn.4146>
31. Lindsey ML, Bolli R, Cauty JM Jr, Du XJ, Frangogiannis NG, Frantz S, Gourdie RG, Holmes JW, Jones SP, Kloner RA, Lefer DJ, Liao R, Murphy E, Ping P, Przyklenk K, Recchia FA, Schwartz Longacre L, Ripplinger CM, Van Eyk JE, Heusch G (2018) Guidelines for experimental models of myocardial ischemia and infarction. *Am J Physiol Heart Circ Physiol* 314:H812–H838. <https://doi.org/10.1152/ajpheart.00335.2017>
32. Loffredo FS, Steinhauser ML, Jay SM, Gannon J, Pancoast JR, Yalamanchi P, Sinha M, Dall'Osso C, Khong D, Shadrach JL, Miller CM, Singer BS, Stewart A, Psychogios N, Gerszten RE, Hartigan AJ, Kim MJ, Serwold T, Wagers AJ, Lee RT (2013) Growth differentiation factor 11 is a circulating factor that reverses age-related cardiac hypertrophy. *Cell* 153:828–839. <https://doi.org/10.1016/j.cell.2013.04.015>
33. Ma S, Wang Y, Chen Y, Cao F (2015) The role of the autophagy in myocardial ischemia/reperfusion injury. *Biochim Biophys Acta* 1852:271–276. <https://doi.org/10.1016/j.bbadis.2014.05.010>
34. Marinkovic D, Zhang X, Yalcin S, Luciano JP, Brugnara C, Huber T, Ghaffari S (2007) Foxo3 is required for the regulation of oxidative stress in erythropoiesis. *J Clin Invest* 117:2133–2144. <https://doi.org/10.1172/jci31807>
35. Matsui Y, Takagi H, Qu X, Abdellatif M, Sakoda H, Asano T, Levine B, Sadoshima J (2007) Distinct roles of autophagy in the heart during ischemia and reperfusion: roles of AMP-activated protein kinase and Beclin 1 in mediating autophagy. *Circ Res* 100:914–922. <https://doi.org/10.1161/01.RES.0000261924.76669.36>
36. Miyazono K (2000) Positive and negative regulation of TGF-beta signaling. *J Cell Sci* 113(Pt 7):1101–1109
37. Morciano G, Giorgi C, Bonora M, Punzetti S, Pavesani R, Wieckowski MR, Campo G, Pinton P (2015) Molecular identity of the mitochondrial permeability transition pore and its role in ischemia-reperfusion injury. *J Mol Cell Cardiol* 78:142–153. <https://doi.org/10.1016/j.yjmcc.2014.08.015>
38. Mozaffari MS, Liu JY, Abebe W, Baban B (2013) Mechanisms of load dependency of myocardial ischemia reperfusion injury. *Am J Cardiovasc Dis* 3:180–196
39. Opstad TB, Seljeflot I, Bohmer E, Arnesen H, Halvorsen S (2017) MMP-9 and its regulators TIMP-1 and EMMPRIN in patients with acute ST-elevation myocardial infarction: a NORDISTEMI substudy. *Cardiology* 139:17–24. <https://doi.org/10.1159/000481684>
40. Poillet-Perez L, Despouy G, Delage-Mourroux R, Boyer-Guittaut M (2015) Interplay between ROS and autophagy in cancer cells, from tumor initiation to cancer therapy. *Redox Biol* 4:184–192. <https://doi.org/10.1016/j.redox.2014.12.003>
41. Rabinowitz JD, White E (2010) Autophagy and metabolism. *Science* 330:1344–1348. <https://doi.org/10.1126/science.1193497>
42. Rochette L, Zeller M, Cottin Y, Vergely C (2015) Growth and differentiation factor 11 (GDF11): functions in the regulation of erythropoiesis and cardiac regeneration. *Pharmacol Ther* 156:26–33. <https://doi.org/10.1016/j.pharmthera.2015.10.006>
43. Saito T, Rodger IW, Shennib H, Hu F, Tayara L, Giaid A (2003) Cyclooxygenase-2 (COX-2) in acute myocardial infarction: cellular expression and use of selective COX-2 inhibitor. *Can J Physiol Pharmacol* 81:114–119. <https://doi.org/10.1139/y03-023>
44. Schofield ZV, Woodruff TM, Halai R, Wu MC, Cooper MA (2013) Neutrophils—a key component of ischemia-reperfusion

- injury. *Shock* 40:463–470. <https://doi.org/10.1097/shk.000000000000044>
45. Su HH, Chu YC, Liao JM, Wang YH, Jan MS, Lin CW, Wu CY, Tseng CY, Yen JC, Huang SS (2017) *Phellinus linteus* mycelium alleviates myocardial ischemia-reperfusion injury through autophagic regulation. *Front Pharmacol* 8:175. <https://doi.org/10.3389/fphar.2017.00175>
  46. Traylor A, Hock T, Hill-Kapturczak N (2007) Specificity protein 1 and Smad-dependent regulation of human heme oxygenase-1 gene by transforming growth factor-beta1 in renal epithelial cells. *Am J Physiol Renal Physiol* 293:F885–F894. <https://doi.org/10.1152/ajprenal.00519.2006>
  47. Walker RG, Poggioli T, Katsimpardi L, Buchanan SM, Oh J, Watrus S, Heidecker B, Fong YW, Rubin LL, Ganz P, Thompson TB, Wagers AJ, Lee RT (2016) Biochemistry and biology of GDF11 and myostatin: similarities, differences, and questions for future investigation. *Circ Res* 118:1125–1141. <https://doi.org/10.1161/circresaha.116.308391> (discussion 1142)
  48. Wang J, Hu X, Jiang H (2015) The Nrf-2/ARE-HO-1 axis: an important therapeutic approach for attenuating myocardial ischemia and reperfusion injury-induced cardiac remodeling. *Int J Cardiol* 184:263–264. <https://doi.org/10.1016/j.ijcard.2015.02.073>
  49. Wang YH, Chen KM, Chiu PS, Lai SC, Su HH, Jan MS, Lin CW, Lu DY, Fu YT, Liao JM, Chang JT, Huang SS (2016) Lumbrakinase attenuates myocardial ischemia-reperfusion injury by inhibiting TLR4 signaling. *J Mol Cell Cardiol* 99:113–122. <https://doi.org/10.1016/j.yjmcc.2016.08.004>
  50. Whelan RS, Kaplinskiy V, Kitsis RN (2010) Cell death in the pathogenesis of heart disease: mechanisms and significance. *Annu Rev Physiol* 72:19–44. <https://doi.org/10.1146/annurev.physiol.010908.163111>
  51. WHO (2018) The top 10 causes of death. In: Media Centre World Health Organization. <https://www.who.int/news-room/fact-sheets/detail/the-top-10-causes-of-death>
  52. Yang Y, Yang Y, Wang X, Du J, Hou J, Feng J, Tian Y, He L, Li X, Pei H (2017) Does growth differentiation factor 11 protect against myocardial ischaemia/reperfusion injury? A hypothesis. *J Int Med Res* 45:1629–1635. <https://doi.org/10.1177/0300060516658984>

## Affiliations

Hsing-Hui Su<sup>1</sup> · Juan-Miaw Liao<sup>2</sup> · Yi-Hsin Wang<sup>3</sup> · Ke-Min Chen<sup>4</sup> · Chia-Wei Lin<sup>5</sup> · I-Hui Lee<sup>6,7</sup> · Yi-Ju Li<sup>8,9</sup> · Jing-Yang Huang<sup>3,10</sup> · Shen Kou Tsai<sup>11</sup> · Jiin-Cherng Yen<sup>1</sup> · Shiang-Suo Huang<sup>3,12,13</sup> 

<sup>1</sup> Department and Institute of Pharmacology, School of Medicine, National Yang-Ming University, No. 155, Sec. 2, Lih-Nong Street, Taipei 11221, Taiwan

<sup>2</sup> Department of Physiology, Chung Shan Medical University and Chung Shan Medical University Hospital, Taichung, Taiwan

<sup>3</sup> Institute of Medicine, Chung Shan Medical University, Taichung, Taiwan

<sup>4</sup> Department of Parasitology, Chung Shan Medical University, Taichung, Taiwan

<sup>5</sup> Institute of Biochemistry, Microbiology and Immunology, Medical College of Chung Shan Medical University, Taichung, Taiwan

<sup>6</sup> Department of Neurology, Taipei Veterans General Hospital, Taipei, Taiwan

<sup>7</sup> Institute of Brain Science, National Yang-Ming University, Taipei, Taiwan

<sup>8</sup> Department of Pathology, Chung Shan Medical University, Taichung, Taiwan

<sup>9</sup> Department of Pathology, Chung Shan Medical University Hospital, Taichung, Taiwan

<sup>10</sup> Department of Medical Research, Chung Shan Medical University Hospital, Taichung, Taiwan

<sup>11</sup> Cheng-Hsin General Hospital, No 45, Cheng Hsin St, Beitou, Taipei, Taiwan

<sup>12</sup> Department of Pharmacology, Chung Shan Medical University, No. 110, Sec. 1, Jianguo N. Rd., Taichung 402, Taiwan

<sup>13</sup> Department of Pharmacy, Chung Shan Medical University Hospital, No. 110, Sec. 1, Jianguo N. Rd., Taichung 402, Taiwan